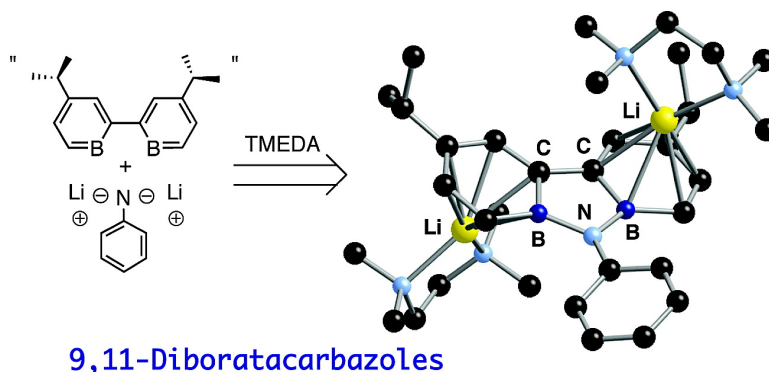


Lewis Acid Chelation of [NR] by 2,2'-Diborabiphenyl: 9,11-Diboratacarbazole Heterocycles

Ioan Ghesner, Warren E. Piers, Masood Parvez, and Robert McDonald

Organometallics, 2004, 23 (13), 3085-3087 • DOI: 10.1021/om049800z

Downloaded from <http://pubs.acs.org> on December 12, 2008



More About This Article

Additional resources and features associated with this article are available within the HTML version:

- Supporting Information
- Links to the 5 articles that cite this article, as of the time of this article download
- Access to high resolution figures
- Links to articles and content related to this article
- Copyright permission to reproduce figures and/or text from this article

[View the Full Text HTML](#)

Lewis Acid Chelation of $[NR]^{2-}$ by 2,2'-Diborabiphenyl: 9,11-Diboratacarbazole Heterocycles

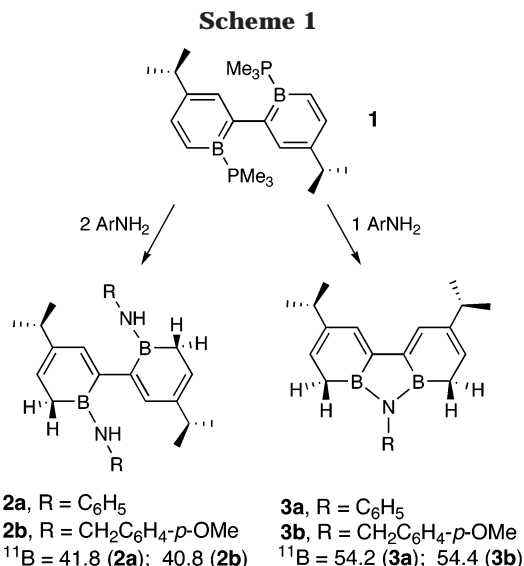
Ioan Ghesner,[†] Warren E. Piers,^{*,†} Masood Parvez,[†] and Robert McDonald[‡]

Department of Chemistry, University of Calgary, 2500 University Drive NW,
Calgary, Alberta, Canada T2N 1N4, and X-ray Structure Laboratory,
Department of Chemistry, University of Alberta, Edmonton, Alberta, Canada T6G 2G2

Received March 18, 2004

Summary: A new heterocyclic framework, the dianionic 9,11-diboratacarbazole, has been prepared from a bis-(trimethylphosphine)-stabilized 2,2'-diborabiphenyl derivative, **1**, and H_2NR ($R = Ph, CH_2C_6H_4-p-OMe$). The heterocyclic framework is formally assembled via Lewis acid chelation of the $[NR]^{2-}$ dianion by 2,2'-diborabiphenyl. These dianions are isoelectronic with the well-studied fluorenyl monoanion.

Transposition of carbon atoms for boron and/or nitrogen in aromatic hydrocarbyl π donors has been a fruitful strategy for the development of new ligands for transition metals with comparable steric properties but altered electronic characteristics.¹ In this way, modifications to the ubiquitous C_5H_5 (Cp) anion have led to isoelectronic borollide² (C_4H_4BR) dianions and monoanionic azaborollide³ (C_3H_3BRNR') donors with applications in olefin polymerization catalysis.⁴ Indenyl,⁵ arene,⁶ and fluorenyl⁷ donors have also been manipulated in this fashion. The fluorenyl ligand framework is also an important one in olefin polymerization catalysis,⁸ but the extended conjugative network also allows for its use as a sensitive chromophore in fluorescent materials.⁹ Thus, in addition to comparative coordination chemistry, the photophysical properties of heterocyclic analogues of the fluorenyl group are also of interest.



Recently, we reported a route to two synthons for the chelating Lewis acid 2,2'-diborabiphenyl, which was shown to bind bifunctional pyridazine Lewis bases, giving B_2N_2 analogues of polycyclic aromatic hydrocarbons.¹⁰ The $[NR]^{2-}$ fragment constitutes the simplest bifunctional, nitrogen-based donor, and chelation of $[NR]^{2-}$ by this Lewis acid would lead directly to a dianionic B_2N analogue of the fluorenyl anion.

The 2,2'-diborabiphenyl synthon **1** was used to prepare precursors to the 9,11-diboratacarbazole framework, as shown in Scheme 1. Base-stabilized borabenzene derivatives are known to undergo reaction with protic acids via addition of $E-H$ across the $B=C$ bond of the borabenzene framework;¹¹ deprotonation of the resultant cyclic borane provides a facile route to boratabenzenes. This methodology was applied using aniline and *p*-methoxybenzylamine as the protic acids. Addition of 2 equiv of H_2NAr to **1** occurs smoothly at room temperature to give the colorless bis(amido)boranes **2**, but when only 1 equiv of aniline or amine is employed, ring closure via addition of the second aniline or amine proton to the other half of the diborabiphenyl molecule can be achieved at higher temperatures and longer reaction times to give the tricyclic B_2N heterocycles **3** in about 60% isolated yield.¹² Observable amounts of compounds **2** are also formed in these reactions and do not thermally convert to the ring-closed

(10) Emslie, D. J. H.; Piers, W. E.; Parvez, M. *Angew. Chem., Int. Ed.* **2003**, *42*, 1251.

(11) Rogers, J. S.; Lachicotte, R. J.; Bazan, G. C. *J. Am. Chem. Soc.* **1999**, *121*, 1288.

* To whom correspondence should be addressed. Phone: 403-220-5746. E-mail: wpiers@ucalgary.ca. S. Robert Blair Professor of Chemistry (2000–2005).

[†] University of Calgary.

[‡] University of Alberta.

(1) For recent reviews see: (a) Fu, G. C. *Adv. Organomet. Chem.* **2001**, *47*, 101. (b) Herberich, G. E.; Ohst, H. *Adv. Organomet. Chem.* **1986**, *25*, 199. (c) Siebert, W. *Adv. Organomet. Chem.* **1993**, *35*, 187.

(2) Herberich, G. E.; Hostalek, M.; Laven, R.; Boese, R. *Angew. Chem., Int. Ed. Engl.* **1990**, *23*, 317.

(3) (a) Liu, S.-Y.; Lo, M. M.-C.; Fu, G. C. *Angew. Chem., Int. Ed.* **2002**, *41*, 174. (b) Ashe, A. J., III; Fang, X. *Org. Lett.* **2000**, *2*, 2089.

(4) (a) Bazan, G. C.; Donnelly, S. J.; Rodriguez, G. *J. Am. Chem. Soc.* **1995**, *117*, 2671. (b) Pastor, A.; Kiely, A. F.; Henling, L. M.; Day, M. W.; Bercaw, J. E. *J. Organomet. Chem.* **1997**, *528*, 65. (c) Nagy, S.; Krishnamurti, R.; Etherton, B. P. *PCT Int. Appl. W09634-021*; *Chem. Abstr.* **1997**, *126*, 19432j.

(5) Ashe, A. J., III; Yang, H.; Fang, X.; Kampf, J. W. *Organometallics* **2002**, *21*, 4578.

(6) (a) Komon, K. J. A.; Bazan, G. C. In *Contemporary Boron Chemistry*; Davidson, M. G., Highes, A. K., Marder, T. B., Wade, K., Eds.; The Royal Society of Chemistry: Cambridge, U.K., 2000; p 3. (b) Ashe, A. J., III; Al-Ahmed, S.; Fang, X. *J. Organomet. Chem.* **1999**, *581*, 92.

(7) Wehmschulte, R. J.; Khan, M. A.; Twamley, B.; Schiemenz, B. *Organometallics* **2001**, *20*, 844.

(8) (a) Alt, H. G.; Köppl, A. *Chem. Rev.* **2000**, *100*, 1205. (b) Ewen, J. A.; Jones, R. L.; Razavi, A.; Ferrara, J. D. *J. Am. Chem. Soc.* **1988**, *110*, 6255. (c) Dietrich, U.; Hackmann, M.; Rieger, B.; Klinga, M.; Leskelä, M. *J. Am. Chem. Soc.* **1999**, *121*, 4348. (d) Miller, S. A.; Bercaw, J. E. *Organometallics* **2002**, *21*, 934.

(9) Tirapattur, S.; Belletete, M.; Drolet, N.; Leclerc, M.; Durocher, G. *Macromolecules* **2002**, *35*, 8889 and references therein.

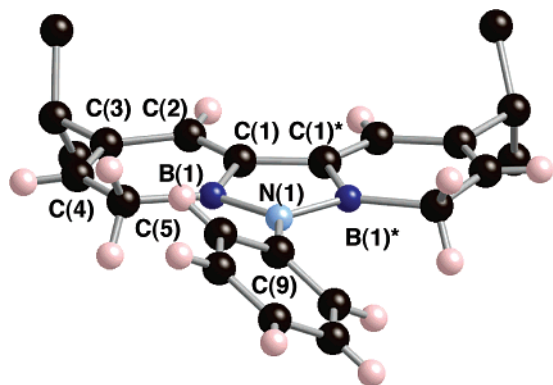


Figure 1. Crystallmaker representation of the structure of **3a**. Isopropyl hydrogen atoms are omitted for clarity. Selected bond lengths (Å): N(1)–B(1), 1.459(2); C(1)–B(1), 1.545(2); C(1)–C(2), 1.351(2); C(2)–C(3), 1.462(2); C(3)–C(4), 1.349(2); C(4)–C(5), 1.504(2); C(5)–B(1), 1.569(2); C(1)–C(1)*, 1.466(3). Selected bond angles (deg): C(9)–N(1)–B(1), 125.71(8); B(1)–N(1)–B(1)*, 108.57(16); C(1)–B(1)–C(5), 117.46(12); N(1)–B(1)–C(5), 133.82(13); N(1)–B(1)–C(1), 108.72(12).

products, indicating that the addition of N–H bonds to the borabenzene unit is irreversible under these conditions. Heterocycles **3** can be separated from compounds **2** via fractional crystallization from isopentane solutions as light yellow solids. All compounds were characterized by NMR and electronic spectroscopy and high-resolution mass spectrometry.¹³ Since the boron centers are three-coordinate aminoboranes, they exhibit a diagnostic resonance at ≈ 41 ppm (**2a,b**) and 54 ppm (**3a,b**) (relative to $\text{BF}_3 \cdot \text{Et}_2\text{O}$ at 0 ppm). In addition, **3a** was characterized by X-ray crystallography.¹⁴

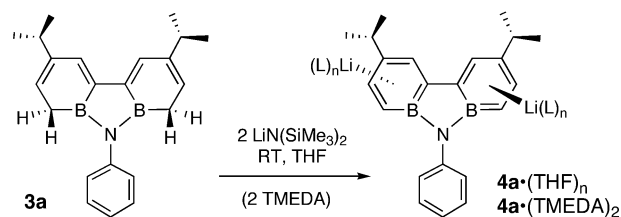
A Crystallmaker diagram of **3a** is shown in Figure 1, along with selected metrical data. Despite the presence of an sp^3 carbon center in the six-membered rings, the atoms of the three cycles are essentially coplanar, with the *N*-phenyl group twisted out of this plane by 34.5° . The B–C bond lengths are in the range found for single

(12) Synthesis of **3a**: aniline (49 mg, 0.52 mmol) in 2 mL of toluene was added at room temperature to a solution of the bis-PMe₃ adduct of 2,2'-diborabiphenyl (205 mg, 0.53 mmol) in 4 mL of toluene. The solution was stirred for 20 h at 65°C , and the volatiles were removed under vacuum. The product was obtained as a light yellow solid after recrystallization from isopentane at -35°C (110 mg, 63%). Mp: 155°C . ^1H NMR (C_6D_6 , 400 MHz): δ 1.28 (d, 12H, CH_3 Pr, $^3J_{\text{HH}} = 6.9$ Hz), 2.12 (d, 4H, BClH_2 , $^3J_{\text{HH}} = 4.2$ Hz), 2.65 (sept, 2H, CH Pr, $^3J_{\text{HH}} = 6.7$ Hz), 6.02 (t, 2H, CH^p , $^3J_{\text{HH}} = 4.4$ Hz), 7.03 (m, 2H, C_6H_5 ortho or meta), 7.09 (m, 1H, C_6H_5 para), 7.24 (m, 2H, C_6H_5 ortho or meta), 7.50 (d, 2H, CH^o , $^4J_{\text{HH}} = 0.9$ Hz). $^{13}\text{C}\{^1\text{H}\}$ NMR (C_6D_6 , 100 MHz): δ 20.10 (s, BC^oH_2), 22.72 (s, CH_3 Pr), 35.41 (s, CH Pr), 124.02 (s, C_6H_5 ortho or meta), 124.62 (s, C_6H_5 para), 124.91 (s, CH^o), 129.22 (s, C_6H_5 ortho or meta), 134.48 (s, CH^o), 141.24 (s, br, C ipso), 144.18 (s, C ipso), 145.94 (s, C ipso). ^{11}B NMR (C_6D_6 , 128 MHz): δ 54.15 (br). EI-MS: m/z 327 [M^+], 284 [$\text{M}^+ - \text{CH}(\text{CH}_3)_2$], 242 [$\text{M}^+ - 2 \text{CH}(\text{CH}_3)_2$], 43 [$\text{CH}(\text{CH}_3)_2^+$]. EI-HRMS: m/z 327.232 13 (calcd 327.232 96 amu, $\text{C}_{22}\text{H}_{27}\text{N}^{11}\text{B}_2$). UV/vis (THF): λ_{max} nm (ϵ) 364 br (15 414), 324 sh (11 986), 276 sh (13 736), 244 sh (22 224), 221 (25 987). Fluorescence emission (THF): λ_{max} nm ($\lambda_{\text{excitation}}$ 242 nm) 333, 485, 664.

(13) See the Supporting Information.

(14) Crystallographic data for $\text{C}_{22}\text{H}_{27}\text{B}_2\text{N}$: monoclinic, space group $C2/c$, radiation Mo $\text{K}\alpha$ ($\lambda = 0.710 73$ Å), $a = 20.924(7)$ Å, $b = 11.808(5)$ Å, $c = 7.700(3)$ Å, $\beta = 99.47(3)^\circ$, $V = 1876.5(12)$ Å³, $Z = 4$, absorption coefficient 0.065 mm^{-1} , $F(000) = 704$, crystal size $0.16 \times 0.10 \times 0.4 \text{ mm}^3$, $T = 173(2)$ K, θ range for data collection $3.4\text{--}27.5^\circ$, index range $-27 \leq h \leq 27$, $-15 \leq k \leq 13$, $-9 \leq l \leq 9$, 3725 reflections collected, 2136 independent reflections ($R(\text{int}) = 0.031$), completeness to $\theta = 27.5^\circ$ 99.3%, absorption correction multiscan method, refinement method full-matrix least squares on F^2 , number of data/restraints/parameters 2136/0/117, goodness of fit on F^2 1.01, final R indices ($I > 2\sigma(I)$) $R1 = 0.046$ and $wR2 = 0.106$, final R indices (all data) $R1 = 0.076$ and $wR2 = 0.121$, largest difference peak and hole $0.19/-0.17 \text{ e } \text{Å}^{-3}$.

Scheme 2



bonds, while the C–C bonds of the flanking six-membered rings alternate between short (C(1)–C(2) and C(3)–C(4)) and long (C(2)–C(3) and C(4)–C(5)), indicating localization of π bonds in this system.

Double deprotonation of the heterocycle **3a** with a lithium amide base leads to the dianionic 9,11-diboratacarbazole derivative **4a**·*n*THF (Scheme 2).¹⁵ Reaction is rapid and quantitative at room temperature and is signaled in the ^{11}B NMR spectrum by a significant upfield shift from ~ 54 to 31.7 ppm, characteristic of an amido-substituted boratabenzene moiety.⁷ ^7Li NMR spectroscopy in THF reveals a signal at -6.1 ppm relative to external LiCl, which is indicative of a contact ion pair in which the Li is interacting with the π system of an aromatic ring.¹⁶ The resonance remains unchanged at all accessible temperatures, indicating a symmetrical structure, but a fast exchange of the lithium ions between flanking rings cannot be excluded.

Crystals of **4a**·*n*THF were not of X-ray quality, but treatment with 2 equiv of TMEDA (*N,N,N,N*-tetramethylethylenediamine) followed by crystallization from toluene/isopentane afforded good-quality single crystals of the bis-TMEDA adduct **4a**·2TMEDA·PhMe (Figure

(15) Synthesis of **4a**·THF: lithium bis(trimethylsilyl)amide (60 mg, 0.36 mmol) in 4 mL of THF was added dropwise to a THF solution (6 mL) of **3a** (59 mg, 0.18 mmol) at room temperature. The mixture was further stirred for 10 min at room temperature, and the volatiles were removed under vacuum. The product was obtained as a yellow solid after washing with pentane (60 mg, 98%). Dec pt: 163°C . For crystallization purposes *N,N,N,N*-tetramethylethylenediamine was added to a solution of **4a**·THF in THF, the mixture was stirred for 30 min at room temperature, and the volatiles were removed under vacuum. Single crystals were grown by cooling a solution of **4a**·2TMEDA in toluene/isopentane at -35°C . ^1H NMR (THF- d_6 , 400 MHz): δ 1.30 (d, 12H, CH_3 Pr, $^3J_{\text{HH}} = 6.9$ Hz), 1.78 (m, 4H, CH_2 THF), 2.89 (sept, 2H, CH Pr, $^3J_{\text{HH}} = 6.9$ Hz), 3.62 (m, 4H, CH_2 THF), 6.25 (d, 2H, CH^p , $^3J_{\text{HH}} = 10.3$ Hz), 6.52 (t, 1H, C_6H_5 para, $^3J_{\text{HH}} = 7.1$ Hz), 7.08 (m, 4H, C_6H_5 ortho + CH^o), 7.63 (s, br, 2H, CH^o), 7.76 (d, 2H, C_6H_5 meta, $^3J_{\text{HH}} = 8.3$ Hz). $^{13}\text{C}\{^1\text{H}\}$ NMR (THF- d_6 , 100 MHz): δ 26.54 (s, CH_2 THF), 26.61 (s, CH_3 Pr), 36.41 (s, CH Pr), 68.38 (s, CH_2 THF), 107.79 (s, CH^i), 116.38 (s, C_6H_5 para), 117.78 (s, CH^i), 122.50 (s, CH ortho), 123.29 (s, C ipso), 128.51 (s, C_6H_5 meta), 128.86 (s, CH^o), 138.90 (s, br, C ipso), 155.57 (s, C ipso). ^{11}B NMR (THF- d_6 , 128 MHz): δ 31.71 (br). ^7Li NMR (THF- d_6 , 155 MHz): δ -6.08 (s). ESI-MS: m/z 338 [**4a**Li₂ – H⁺]. UV/vis (THF): λ_{max} nm (ϵ) 509 br (3259), 343 sh (8763), 278 sh (11 580), 249 (19 735). Fluorescence emission (THF): λ_{max} nm ($\lambda_{\text{excitation}}$ 404 nm) 496.

(16) (a) Elschenbroich, C.; Salzer, A. *Organometallics: A Concise Approach*, 2nd ed.; VCH: Weinheim, Germany, 1992; pp 24–27. (b) Dixon, J. A.; Gwinner, P. A.; Lini, D. C. *J. Am. Chem. Soc.* **1965**, *87*, 1379.

(17) Crystallographic data for $\text{C}_{34}\text{H}_{57}\text{B}_2\text{Li}_2\text{N}_5\text{C}_7\text{H}_8$: monoclinic, space group $P2_1/n$ (an alternate setting of $P2_1/c$ [No. 14]), radiation Mo $\text{K}\alpha$ ($\lambda = 0.710 73$ Å), $a = 18.9342(14)$ Å, $b = 11.7733(9)$ Å, $c = 19.3032(15)$ Å, $\beta = 101.2639(18)^\circ$, $V = 4220.1(6)$ Å³, $Z = 4$, absorption coefficient 0.060 mm^{-1} , crystal size $0.27 \times 0.21 \times 0.20 \text{ mm}^3$, $T = 193$ K, 2θ range for data collection $4.42\text{--}51.62^\circ$, index range $-23 \leq h \leq 22$, $-14 \leq k \leq 14$, $-24 \leq l \leq 23$, 28 615 data collected, 8627 independent reflections ($R(\text{int}) = 0.1179$), absorption correction multiscan (SADABS), refinement method full-matrix least squares on F^2 (SHELXL-93), number of data/restraints/parameters 8627 ($F_o^2 \geq -3\sigma(F_o^2)$)/0/452, goodness of fit on S 0.976 ($F_o^2 \geq -3\sigma(F_o^2)$), final R indices $R1 = 0.0727$ ($F_o^2 \geq 2\sigma(F_o^2)$) and $wR2 = 0.2342$ ($F_o^2 \geq -3\sigma(F_o^2)$), largest difference peak and hole $0.422/-0.241 \text{ e } \text{Å}^{-3}$.

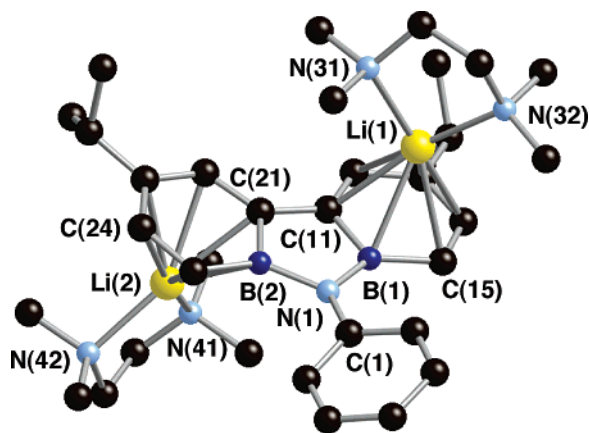


Figure 2. Crystalmaker representation of the structure of **4a**·2TMEDA·PhMe. Hydrogen atoms are omitted for clarity. Selected bond lengths (Å): N(31)–Li(1), 2.105(6); N(32)–Li(1), 2.144(6); C(11)–Li(1), 2.368(6); C(12)–Li(1), 2.365(6); C(13)–Li(1), 2.353(6); C(14)–Li(1), 2.358(6); C(15)–Li(1), 2.417(6); N(1)–B(1), 1.474(4); N(1)–B(2), 1.485(4); C(15)–B(1), 1.516(5); C(25)–B(2), 1.514(5); C(11)–B(1), 1.521(5); C(21)–B(2), 1.518(4); C(11)–C(21), 1.483(4); N(1)–C(1), 1.402(4). Selected bond angles (deg): C(1)–N(1)–B(1), 126.4(3); C(1)–N(1)–B(2), 125.9(3); B(1)–N(1)–B(2), 107.1(2); N(1)–B(1)–C(15), 136.6(3); N(1)–B(1)–C(11), 109.6(3).

2).¹⁷ The lithiums are associated with the flanking six-membered rings above and below the 9,11-boratacarbazole plane and are asymmetrically bonded to the various atoms of the ring. In particular, the Li–B distances of 2.456(7) and 2.497(6) Å are somewhat longer than the Li–C distances, which range from 2.316(6) to 2.417(6) Å. Distances and angles within the C₁₀B₂N ring are similar to those in **3a**, with the exception of the C–C distances, which are now more equalized due to the rearomatization of these rings.

Computational exploration of the diboratacarbazole's electronic structure at the 3-21G level using Spartan

'02 indicates that the HOMO is largely associated with the flanking six-membered rings rather than the B₂C₂N core, whereas the HOMO-1 has substantial contributions from all of the atoms in the C₁₀B₂N framework.¹³ The energetic ordering of these two orbitals is reversed in the electrostatic potential maps for the two compounds,¹³ as the two anionic charges in the 9,11-diboratacarbazole framework avoid each other on the peripheral rings of the C₁₀B₂N tricycle. These observations suggest that η^6 bonding can be expected to dominate in the coordination chemistry of **4a** with transition metals, as the η^5 mode is emphasized in the coordination chemistry of the fluorenyl anion.⁹ On the other hand, the energy surface between η^5 and η^6 bonding in the fluorenyl anion is somewhat soft,¹⁸ and given the similarly close energies of the highest energy orbitals in the diboratacarbazole dianion, analogous flexibility in bonding modes might be expected here. We are therefore currently exploring the coordination chemistry of these novel heterocycles, as well as their electronic structure through spectroscopic studies.

Acknowledgment. Funding for this work was provided by the NSERC of Canada through a Discovery grant to W.E.P. and the Alberta Ingenuity Fund for an Associateship to I.G.

Supporting Information Available: Text, tables, and figures giving experimental details, crystal data, atomic coordinates, bond lengths and angles, ORTEP diagrams, and anisotropic displacement parameters for **3a** and **4a**·2TMEDA·PhMe and details on the computations; X-ray data for **3a** and **4a**·2TMEDA·PhMe are also available as CIF files. This material is available free of charge via the Internet at <http://pubs.acs.org>.

OM049800Z

(18) (a) Johnson, J. W.; Treichel, P. M. *J. Am. Chem. Soc.* **1977**, *99*, 1427. (b) Üffing, C.; Köppe, R.; Schnöckel, H. *Organometallics* **1998**, *17*, 3512.